The Amnesic Shellfish Poisoning toxin, domoic acid: the tattoo of the king scallop Pecten maximus

José Luis García-Corona, Caroline Fabioux, Jean Vanmaldergem, Sylvain Petek, Amélie Derrien, Aouregan Terre-Terrillon, Laura Bressolier, Florian Breton, Hélène Hegaret

The Amnesic Shellfish Poisoning toxin, domoic acid: the tattoo of the king scallop *Pecten maximus*

José Luis García-Corona[1], Caroline Fabioux[1], Jean Vanmaldergem[1], Sylvain Petek[1], Amélie Derrien[2], Aouregan Terre-Terrillon[2], Laura Bressolier[1], Florian Breton[3] & Hélène Hegaret[1*]

[1]Institut Universitaire Européen de la Mer, Laboratoire des Sciences de l'Environnement Marin, UMR 6539 LEMAR UBO, CNRS, IRD, Ifremer, F-29280 Plouzané, France.

[2]Ifremer, LITTORAL LER BO, Station de Biologie Marine, Place de la Croix, BP40537, 29900 Concarneau Cedex, France.

[3]Écloserie du Tinduff, 148 rue de l'écloserie, Port du Tinduff, 29470, Plougastel-Daoulas, France.

*Corresponding author: Hélène Hegaret

Institut Universitaire Européen de la Mer, Laboratoire des Sciences de l'Environnement Marin, UMR 6539 LEMAR UBO, CNRS, IRD, Ifremer, F-29280 Plouzané, France.

e-mail: helene.hegaret@univ-brest.fr

Abstract

Domoic acid (DA) is a potent neurotoxin produced by diatoms of the genus *Pseudo-nitzschia* and is responsible for Amnesic Shellfish Poisoning (ASP) in humans. Some fishery resources of high commercial value, such as the king scallop *Pecten maximus*, are frequently exposed to toxic *Pseudo-nitzschia* blooms and are capable of accumulating high amounts of DA, retaining it for months or even a few years. This poses a serious threat to public health and a continuous economical risk due to fishing closures of this resource in the affected areas. Recently, it was hypothesized that trapping of DA within autophagosomic-vesicles could be one reason explaining the long retention of the remaining toxin in *P. maximus* digestive gland. To test this idea, we follow the kinetics of the subcellular localization of DA in the digestive glands of *P. maximus* during (a) the contamination process — with sequential samplings of scallops reared in the field during 234 days and naturally exposed to blooms of DA-producing *Pseudo-nitzschia australis*, and (b) the decontamination process — where highly contaminated scallops were collected after a natural bloom of toxic *P. australis* and subjected to DA-depuration in the laboratory for 60 days. In the digestive gland, DA-depuration rate (0.001 day^{-1}) was much slower than contamination kinetics. The subcellular analyses revealed a direct implication of early autophagy in DA sequestration throughout contamination (r = 0.8, P <0.05), while the presence of DA-labeled residual bodies (late autophagy) appeared to be strongly and significantly related to slow DA-depuration (r = -0.5) resembling an analogous DA-tattooing in the digestive glands of *P. maximus*. This work provides new evidence about the potential physiological mechanisms involved in the long retention of DA in *P. maximus* and represents the baseline to explore procedures to accelerate decontamination in this species.

Keywords: domoic acid, *Pecten maximus*, toxicokinetics, rapid accumulation, slow depuration, autophagy.

1. Introduction

Over the last three decades, natural stocks of important fishery resources have been subjected to intense and frequent blooms of toxic diatoms of the genus *Pseudo-nitzschia*, widely distributed throughout all oceans of the world (Hallegraeff 1993; Lelong *et al.*, 2012; Trainer *et al.*, 2012). To date, about 28 species of this genus have been reported to be capable of producing domoic acid (DA), an extremely dangerous amino acid responsible for Amnesic Shellfish Poisoning (ASP) in mammals (Pulido, 2008; La Barre *et al.*, 2014; Bates *et al.*, 2018). The species *P. australis* is frequently reported as one of the most toxigenic of all (Basti *et al.*, 2018; Ayache *et al.*, 2019) and in recent years, its presence has been detected in several countries around the world (Lelong *et al.*, 2012; Bates *et al.*, 2018) including on the northwest coast of France. This represents a threat to the fishing-aquaculture industry due to the numerous persistent harvest closures of shellfish beds (Amzil *et al.*, 2001; Husson *et al.*, 2016; Ayache *et al.*, 2019).

The European Union 2002/226/EC banned shellfish harvesting when DA concentrations exceed the sanitary limit of 20 mg. kg^{-1} of flesh on the whole or individual parts of shellfish (MacKenzie *et al.*, 2002; Wekel *et al.*, 2004) to avoid public health issues. The king scallop *Pecten maximus* is a very valuable fishery resource in the western coast of Europe. In France, this species has an important economic and commercial value (~ 87 million euros yearly); however, the recurrent proliferations of DA-producing *Pseudo-nitzschia* and the subsequent reintoxication episodes of the natural stocks of these resources (Amzil *et al.*, 2001; Husson *et al.*, 2016; Ayache *et al.*, 2019) have led to severe economic losses of nearly 70 million euros per year due to fishery closures (France Filière Pêche: https://www.francefilierepeche.fr/). King scallops have been reported to accumulate less than 6% of total DA burdens in the joint of soft tissues like adductor muscle, gonad, kidney, gills, and mantle, and amounts as high as 3,200 mg. DA kg^{-1} in the digestive gland (> 80% of the total DA) retaining it from several months to even a few years (Blanco *et al.*, 2002a, 2006, 2020). Therefore, the European decision 91/492/EEC allowed the commercialization of *P. maximus* after evisceration of the inedible tissues (i.e. the digestive gland) to reduce the toxin contents (< 4.6 mg. DA kg^{-1} in muscle and gonad) in authorized processing plants.

Many bivalves depurate the toxin quickly, showing decontamination rates of up to 10 day^{-1} in digestive tissues, like some mussels (Wohlgeschaffen *et al.*, 1992; Novaczek *et al.*, 1992; Blanco *et al.*, 2002b; Mafra *et al.*, 2010; Bresnan *et al.*, 2017), clams (Gilgan *et al.*, 1990;

Blanco *et al.*, 2010; Álvarez *et al.*, 2015; Dusek Jennings *et al.*, 2020), and oysters (Jones *et al.*, 1995; Mafra *et al.*, 2010). Some scallops such as *Argopecten purpuratus* are also capable of excreting up to ≥ 80% of total DA-burdens in a few hours, and ~ 90% in a couple of days (Álvarez *et al.*, 2020). On the contrary, other bivalves exhibit slow toxin excretion rates ≤ 0.3 day^{-1} in the digestive gland, as reported for the razor clam *Siliqua patula* (Drum *et al.*, 1993; Horner *et al.*, 1993; Dusek Jennings *et al.*, 2020). Nevertheless, some scallops such as *Placopecten magellanicus* (Wohlgeschaffen *et al.*, 1992; Douglas *et al.*, 1997), and *P. maximus* (Blanco *et al.*, 2002a 2006; Mauríz & Blanco, 2010; Bresnan *et al.*, 2017) show the slowest DA-decontamination kinetics, with rates as slow as 0.05 to 0.007 day^{-1}, respectively, in the digestive gland. It thus appears necessary to better understand the mechanisms associated with this long DA retention.

Physiological mechanisms behind the broad interspecific differences in accumulation and depuration dynamics of DA are still not fully understood. Mauriz and Blanco (2010) suggested that the absence of efficient membrane transporters to excrete the toxin could explain the high accumulation and/or slow depuration of DA in *P. maximus*. Meanwhile, in *A. purpuratus*, the key to the accelerated depuration rates of the toxin could rely on the rapid transfer of most of DA burdens accumulated in the digestive gland to other organs capable to excrete it with greater efficacy (Álvarez *et al.*, 2020). Other mechanisms, such as the expression of low affinity glutamate receptors in all tissues, and the selective activation of high DA capacity sites in tissues such as siphon have been proposed as an explanation for the tissue-specific long retention of ASP toxins in species like *S. patula* (Trainer and Bill, 2004).

Recently, Garcia-Corona *et al.* (2022; 2024) observed, thanks to an immunostaining of DA, that in species like *P. maximus*, *Aequipecten opercularis* (queen scallop), and *Crepidula fornicata* (slipper-limpet), most of the DA staining was trapped within small (~ 1-2.5 µm) autophagic vesicles in the cytoplasm of the digestive cells during active digestion (early autophagy), as well as in remaining post-digestion residual bodies in the distal cytoplasmic zone of digestive cells, undergoing advanced digestion (late autophagy). Nevertheless, none of these hypotheses has been fully elucidated so far. Autophagy is a highly organized and complex intracellular catabolic degradation system well conserved in eukaryotic cells (Owen, 1972, Wang *et al.*, 2019; Zhao *et al.*, 2021). Through this process, the own (*e.g.*, abnormal proteins, excess or damaged organelles) or foreign (*e.g.*, pathogenic microorganisms, chemical compounds) cytoplasmic contents of the cell are digested to recycle energy usable by the cell, or processed for its cell excretion, respectively (Cuervo, 2004; Zheng *et al.*, 2022).

The key structures in autophagy are autophagosomes, spherical vesicles from 0.5 to 2.5 µm in diameter with a double phospholipid membrane (Mizushima *et al.*, 2002). The essential role of autophagy is a key piece in the maintenance of homeostasis and cellular health of bivalves when exposed to potentially toxicological compounds (Moore, 2004; Picot *et al.*, 2019). Harmful algae-derived phycotoxins have recently been demonstrated to trigger autophagic processes in different species of marine invertebrates, but particularly in *P. maximus* contaminated with DA (García-Corona *et al.*, 2022; 2024).

The long retention of exogenous compounds also occurs through macroautophagy, a cellular process analogous to autophagy where mammalian skin macrophages can incorporate and retain tattoo ink into their cytoplasms. These ink-laden macrophages can exhibit lifespans as long as the entire life of the tattooed animal, which explains the long-term tattoo persistence and the difficulties to remove tattoos in mammalian skin cells (Flannagan *et al.*, 2012; Gordon, 2016; Baranska *et al.*, 2018). Hence, we hypothesized that autophagy could be a kind of analogous DA-tattooing mechanism in the digestive glands of *P. maximus*, and one reason explaining the long retention of remaining DA in this species (García-Corona *et al.*, 2022). Notwithstanding, to confirm that autophagy is involved in DA long-term retention, it would be necessary to follow the succession of events that lead to autophagy during the contamination and decontamination process. In this study, the localization of DA within tissues of *P. maximus* during the contamination and decontamination phases, as well as its toxicokinetics and the implication of autophagy was followed thanks to an immunohistochemical time-tracking at the subcellular level, this in order to unveil for how long DA is trapped within these autophagosomic structures.

2. Materials and methods

2.1. Source of scallops and *P. australis* environmental data

A total of 66 scallops *P. maximus* (5.1 ± 0.3 cm shell length, 42.8 ± 8.2 g total weight) were reared in the field within culture-suspended cages at the Lanvéoc cove (48°29'56.3" N, 4°46'29.6" W; Bay of Brest, France) between February and October 2021. The information on the cellular densities of all phytoplankton species, including the DA-producing *Pseudo-nitzschia australis* in the area along the rearing period was obtained from the online database REPHY (REseau d'observation et de surveillance du PHYtoplancton et de l'hydrologie dans les eaux littorales, https://bulletinrephytox.fr/accueil) at the Lanvéoc cove. On March 30, 2021, a bloom of *P. australis* was recorded with densities reaching up to 6×10^4 cells L^{-1} and

lasted for ~15 days. To study the contamination process, sequential sampling of 11 scallops per time point were carried out before the bloom of the toxic *P. australis* mentioned above on February 22, 2021 and March 17, 2021 (corresponding to days 0 and 23 of the sampling, respectively), during the bloom, on March 30, 2021, and April 07, 2021 (corresponding to days 36 and 44 of the sampling, respectively), and after the bloom, on June 26, 2021, and October 14, 2021 (corresponding to days 80 and 234 of the sampling, respectively).

To study the decontamination process, 60 wild scallops (9.7 ± 0.1 cm shell length, 168 ± 6.6 g total weight) were collected by dredging a natural bed in Camaret-sur-Mer, France (48° 26' 33.1"N, 4° 35' 49.6" W) in early April 2021, eight days after the same bloom of *P. australis* mentioned above (~6×10^4 cells L^{-1}, REseau d'observation et de surveillance du PHYtoplancton et de l'hydrologie dans les eaux littorales, https://bulletinrephytox.fr/accueil) to follow depuration of DA at laboratory.

2.2. Depuration of DA in the laboratory and scallop dissection

Scallops naturally contaminated with DA were transported to the Tinduff hatchery (Plougastel-Daoulas, France) within a few hours after collection. Upon arrival at the aquaculture facilities, the organisms were washed and scrubbed of epibionts, and immediately distributed in two 800 L fiberglass tanks (30 scallops. $tank^{-1}$) with a sandy bottom. Filtered seawater (1 µm, activated carbon) was supplied and renewed in the thanks at 0.2 L min^{-1} (complete renewal in 24 hours to minimize re-ingestion of feces) through a continuous upstream-flow system with water pumped from the Bay of Brest. Animals were fed daily with a diet consisting of 10×10^9 $cells.scallop^{-1}day^{-1}$ of the flagellate *Tisochrysis lutea*. These food intakes were provided continuously by mixing the phytoplankton with the filtered water supply. Each tank was covered with a canvas and illuminated separately by a LED spotlight bar (NICREW Classic LED Plus 120-150 cm, 1150 lm) placed 1 m above the water surface with a photoperiod set at 12h:12h (light: darkness). During the experiment, the water was maintained fully oxygenated (100% O_2 saturated) and at a constant temperature of 15.9 °C, and salinity of the pumped seawater within the Bay (*i.e.* between 32.5 and 34 PSU over the 2 months of the experiment). The scallops were maintained under these experimental conditions for 60 days, with sequential sampling of 10 animals after 0, 7, 14, 21, 30, and 60 days of depuration in the laboratory.

All sampled scallops were placed on a frozen plate to avoid suffering during sacrifice. The flesh was carefully excised from the shells, and since the digestive gland (DG) accumulates ≥

80% of the total DA burdens (Blanco *et al.*, 2002a) this organ was carefully dissected and separated from the rest of the tissues (RT = adductor muscle, gills, mantle, kidney, and gonad) to avoid contamination of the other organs by DA of the DG during dissections (García-Corona *et al.*, 2022). The DG of each animal was longitudinally sliced into two halves, one stored at -20 °C to determine the toxin concentration in each individual, and the other fixed in Davidson solution (Kim *et al.*, 2006) for anti-DA immunohistochemical purposes. The rest of the tissues were only stored in Davidson solution for anti-DA inmunohistochemical purposes.

2.3. Domoic acid extraction and analysis

Toxin was extracted exclusively from frozen DG of each scallop following the procedure described by Quilliam *et al.* (1989) with modifications. Approximately 200 mg of tissue homogenate was placed in a 2-mL Eppendorf tube containing 250 mg of glass beads (100–250 µm diameter). Subsequently, 450 µL of MeOH:H_2O (1:1, *v/v*) was added. The sample was ground using a Laboratory Mixer Mill MM 400 system (Retsch® Fisher Scientific, Illkirch-Graffenstaden, FR) for 3 min at 30 Hz then centrifuged for 5 min at 15,000 *g*. The supernatant was then transferred to a 1 mL volumetric flask. This operation was repeated, then the two supernatants were combined in the flask, and the volume was adjusted to 1 mL with MeOH:H_2O (1:1, *v/v*). Then, 800 µL of the crude extract were filtered through 1 mL 0.2 µm nylon centrifugal filters (VWR International, Radnor, PA, USA) at 10,000 *g* for 5 min at 4 °C, and aliquots of 200-µL the filtered extract were stored at -20 °C until analysis.

DA quantification was performed by HPLC-UV according to García-Corona *et al.* (2022) with modification, using an Agilent (Santa Clara, CA, USA) 1260 Infinity LC system (pump, refrigerated autosampler, column oven, diode array detector). Chromatographic separation was carried out on a reversed-phase column Uptisphere TP C_{18} (250 × 4.6 mm, 5 µm, 300 Å, Interchim, Montluçon, France) with an isocratic mobile phase consisting of H_2O + CH_3CN (9:1 *v/v*) with 0.1% of CF_3CO_2H. The flow rate was 1 $mL.min^{-1}$ and the column temperature was maintained at 40 °C. The wavelength was set at 242 nm. The injection volume was 20 µL. The quantification was performed relative to the DA standard (National Research Council Canada, NRCC) with a 5-point calibration curve over the concentration range 0.5 to 10.3 $\mu g.mL^{-1}$. The Limit of Quantification (LOQ) and the Limit of Detection (LOD) of the method were 0.04 and 0.1 $\mu g.m^{-1}$, respectively, which corresponded to 0.2 and 0.5 mg $DA.kg^{-1}$ tissue, respectively.

2.4. Quantitative anti-DA immunohistochemistry

In order to follow the *in situ* localization of the toxin at the subcellular level in the tissues (digestive gland, gills, mantle, adductor muscle, kidney, and gonad) of the scallops in both contamination and decontamination scenarios, a specific anti-DA immunohistochemical protocol recently developed by García-Corona *et al.* (2022) was applied in this work with minor modifications. Paraffin tissue sections (4-µm thickness) were rehydrated and incubated overnight with a dilution (0.01 mg. mL^{-1}) of a Goat polyclonal anti-DA primary antibody (Eurofins Abraxis®, Warminster, PA, USA) at 4°C. The next day, the slides were incubated at 37 °C for 2 h with a dilution (0.001 mg. mL^{-1}) of an HRP sharped IgG Rabbit anti-Goat secondary antibody (abcam®, Cambridge, UK). Finally, samples were revealed with diaminobenzidine (DAB+ Chromogen Substrate Kit, abcam®, Cambridge, UK) for 1 h in darkness at room temperature.

The qualitative description of DA localization in the digestive gland was made considering the development stages of the digestive diverticula of the DG of *P. maximus* according to Mathers (1976) (Fig. 1) as: (A) digestive diverticulum in a holding condition (Hd); cubical digestive cells (dc) with few vacuoles (v) lining a large lumen (l) with secretory cells (sc) easily identified. (B) diverticulum in absorptive condition (Ad); where few vacuoles (v) are present in the apical region of the digestive cells (dc). (C) diverticulum in digestive condition (Dd); where large digestive cells (dc) constitute the tubular region (tr) of the diverticula. (D) diverticulum in advanced digestive condition (ADd); secretory cells (sc) are absent, the digestive cells (dc) constitute the tubular region (tr) while the adipocyte-like cells (al) compose the ascinar region (ar) of the diverticula. (E) diverticulum undergoing breakdown (Bd); digestive cells (dc) show loss of structure and form in the ascinar region (ar) with abundant adipocyte-like cells (al). (F) diverticulum showing regeneration (Rd); the secretory cells (sc) are again visible at the junctions between the old (ascinar region) and new (tubular region) diverticulum.

Three regions from each histological section of the digestive glands treated with the anti-DA immunohistochemical protocol were randomly digitized at high resolution (63× magnification; 600 dpi) using a Nikon D7500 DSLR camera connected to a Zeiss Axio Observer Z1 light microscope (St Louis, MO, USA). The recorded images were processed using the image analysis software Image Pro Plus, v. 4.5 (Media Cybernetics, Bethesda, MD). In García-Corona *et al.* (2022), DA was mainly localized in structures identified as autophagosomes and residual bodies in the cytoplasm of digestive cells. Therefore, a total of 378 micrographs (i.e. 3 micrographs from the DG of each scallop) were used to count the

number of total and positive DA-immunostained autophagosomes, as well as the number of total and anti-DA stained residual bodies present in a predetermined area of ~1.33 mm^2 (García-Corona *et al.*, 2024). Then, calculations of the occurrence of early and late DA-autophagy in the DG of each scallop through contamination and depuration processes were performed according to the following formulas, respectively:

$$DA\ early\ autophagy\ (\%) = \frac{anti - DA\ stained\ autophagosomes}{total\ number\ of\ autophagosomes} \times 100$$

$$DA\ late\ autophagy\ (\%) = \frac{anti - DA\ stained\ residual\ bodies}{total\ number\ of\ residual\ bodies} \times 100$$

2.5. Statistical analysis

Separate one-way analyses of variance (ANOVA, type II Sum of Squares) were applied to determine statistically significant differences in toxin concentrations in the tissues, as well as in the frequencies of early and late autophagy of DA in the DG of the scallops. *A priori* Anderson-Darling and Fligner-killeen tests were applied to confirm the normality of frequencies and homogeneity of variances of the residuals of the data, respectively (Hector, 2015). When needed, data were transformed (log, $1/\chi$, or $\sqrt{\chi}$) prior to analysis to meet *a priori* assumptions. The percentage-expressed values were also arcsine (arcsine $\sqrt{P}$) transformed (Zar, 2010), but all data are reported untransformed as the mean ± standard error (SE) except when indicated. As needed, *post hoc* comparisons of means with Tukey's honest significance test (HSD) were performed to identify differences between means (Hector, 2015; Zar, 2010). Pearson's correlation coefficients were run to assess the relationship between DA burdens and the formation of autophagosomes and residual bodies in the DG of the animals during contamination and decontamination process (Zar, 2010). Since the presence of toxic *P. australis* was continuously observed throughout the field monitoring, DA depuration rate was assessed only in the DG of experimental scallops maintained in the laboratory over the entire 2-month decontamination period. Depuration rate was calculated according to Dusek Jennings *et al.* (2020) using the one-compartment exponential decay model, $DA_t = DA_0 \cdot e^{-rt}$, where DA_t is the DA concentration after t days, DA_0 represents DA concentration at the end of the depuration, t is days elapsed, and the slope of the equation (r) is the daily depuration rate. DA_0 and the slope were estimated using linear regression after ln-transformation of DA burdens (Álvarez *et al.*, 2020), but untransformed data are presented. All data were analyzed

with a level of statistical significance set at $\alpha = 0.05$ using command lines in the R language (R v. 4.2.2, R Core Team, 2020).

3. Results

3.1. Toxin accumulation and depuration

Changes in DA concentrations in the DG of scallops through the natural contamination process are shown in Fig. 2A. The significantly lower toxin burdens in this organ were recorded at the beginning of our monitoring (day 0), with 11.3 ± 1.3 mg DA. kg^{-1}; this value slightly increased (51.2 ± 3.9 mg DA. kg^{-1}, $P < 0.05$) after 23 days of monitoring and following an exposure to a concentration of 800 cells L^{-1} of the toxic *P. australis*. Nonetheless, the contamination rate of scallops peaked abruptly and significantly between 36 and 44 days after our first sampling during a *P. australis* bloom (6×10^4 and 2.1×10^4 cells L^{-1}, respectively recorded from March 30 to April 07, 2021) with average burdens of ~700 mg DA. kg^{-1} in the DG of the scallops. Moreover, the highest interindividual variability in DA accumulation was also observed through this period as evidenced by the high coefficients of variation (CV, 31.8-28.6 %), and with values ranging from 86.5 up to 1,806.8 mg DA. kg^{-1}. Although *P. australis* populations drastically decreased until disappearing after 80 days, scallops remained strongly contaminated (290.2 ± 83.5 mg DA. kg^{-1}). At the last sampling point, 234 days after the first sampling, *i.e.* 198 days after the first bloom, the concentrations of DA in the DG of the animals were close to 32.3 ± 4.5 mg DA. kg^{-1}, Fig. 2A.

The depuration experiment in the laboratory started with heavily contaminated scallops, with concentrations at ~2000 mg DA. kg^{-1} in the DG. Toxin burdens however did not significantly decrease throughout the following 30 days. Even with a slight reduction ($P < 0.05$) of toxin amounts in the DG between 30 and 60 days, the scallops were still highly contaminated (1182.5 ± 105.9 mg DA. kg^{-1}) (Fig 2B). As seen in Fig. 2B, DA depuration rate in the DG of the scallops was estimated at 0.001 day^{-1} from a one-compartment exponential decay model that explained 52% of the variance, with a good statistical fit ($P < 0.05$) and without evidence of over-dispersion of the data.

3.2.Domoic acid *in situ* localization in a contamination and decontamination scenario

The presence of DA was readily detected in the DG of scallops through a natural contamination process (Fig. 2A and Fig. 3). As observed in Fig. 3A, the DA-chromogenic signal appeared since day 0 of the field monitoring trapped within few early autophagosomes

(ea) of small size (~1-2.5 µm) distributed in the apical region of the cytoplasm of the digestive cells (dc), particularly in the digestive diverticula (dd) in absorptive (Ad) condition. Bigger residual bodies (rb) of ~5-10 µm and present only in the adipocyte-like cells (al) in the ascinar region (ar) of the digestive diverticula undergoing breakdown (Bd) acquired a slight anti-DA staining. During the period of steady contamination (days 23 to 80, Fig. 3B-E), an intense process of early autophagy of the toxin was observed. The appearance of numerous early autophagosomes (ea) with a positive anti-DA signal was detected mainly in the apical zone of the digestive cells in the tubular region (tr) within the digestive diverticula in active (Dd) and advanced (ADd) digestion, as well as the digestive diverticula undergoing breakdown (Bd) or showing regeneration (Rd). The formation of late autophagosomes (la) of bigger size (~ 3-5 µm) than early autophagosomes with positive DA-labeling and present in the basal zone of digestive cells was also detected mainly in digestive diverticula in stages of active or advanced digestion, or in the diverticula showing regeneration. Through this period, the presence of some residual bodies with DA-chromogenic signal also occurred in the digestive diverticula undergoing breakdown or regeneration. Finally, at the end of the contamination surveillance (day 234, Fig. 3F), a low prevalence of early autophagosomes was observed in the digestive diverticula in absorption condition, while a high number of residual bodies with an intense anti-DA signal were found widely distributed in the DG of scallops.

On the other hand, in the laboratory DA-depuration scenario, a strong process of early (ea) and late autophagy (la) of the toxin was already activated in highly contaminated scallops since day 0, mainly in digestive diverticula in advanced digestion (ADd), with only few-dyed residual bodies (rb) in the DG (Fig. 4A). As shown in Figs. 4B-C, over the following 7 to 14 days of DA-depuration, a similar amount (40-50 %) of early and late autophagy of the toxin was observed in the DG of the animals, with the presence of autophagosomes and residual bodies with chromogenic signal mostly in the digestive diverticula showing regeneration (Rd). Notwithstanding, between days 21 and 30 of scallop conditioning, the early autophagy of the toxin was negligible, and it was observed how the labeled late autophagosomes gathered in the digestive diverticula undergoing breakdown to give rise to residual bodies with intense anti-DA signal, that were distributed throughout the DG (Fig. 4D-E). At the end of the toxin depuration period (day 60, Fig. 4F), almost no DA autophagy was observed in the digestive diverticula in absorption stages either, with a high prevalence and intensity of DA-labeling in the residual bodies widely distributed in the DG.

The quantitative IHC analyses allowed to corroborate the overall microanatomical observations described above (Fig. 5). Across natural contamination of scallops during ASP bloom, early DA-autophagy (autophagosomes with DA-chromogenic signal) in the DG increased steadily and significantly from day 0 (36.6 ± 7.6 %) to its highest values on day 44 (74 ± 3 %), then, these frequencies decreased to its lowest values (P <0.05) at the end of the surveillance (25.9 ± 3.2 %) after 234 days (Fig. 5A). Whereas late DA-autophagy frequencies (Fig. 5A) showed slight increases (P <0.05) of stained-residual bodies between 0 days (3.6 ± 2 %) and 44-80 days (28.9 ± 6 %, and 19.5 ± 4.6 %, respectively). However, the amount of stained residual bodies significantly peaked up to its highest frequency (92.8 ± 1.5 %) at the end of the field monitoring. Under this scenario, early DA-autophagy was strongly and directly correlated (r = 0.8, P <0.05) with DA accumulation in the DG, while the relationship between the proliferation of anti-DA autophagosomes and residual bodies was negative and significant but not strong (r = -0.46). The correlation between toxin burdens and DA-stained residual bodies in the DG was low (r = -0.21) and non-significant.

Conversely, as shown in Fig. 5B, an inverse pattern between early and late autophagy was found along DA-depuration process (r = -0.8, P <0.05). The frequencies of IHC-labeled autophagosomes decreased (P <0.05) from 76.2 ± 2.6 % at the beginning of the experiment, to ~ 49.7 % between days 7 and 14, to then continue dropping to the minimum values (P <0.05) of ~ 11.5 % at the end of the experiment. While the amount of residual bodies significantly raised from the start (21.9 ± 3.7 %) to days 7 and 14 (~ 44.5 %) and subsequently peaked at its highest frequencies (~ 88.1 %, P <0.05) at the end of the laboratory depuration. Furthermore, a negative and significant relationship (r = -0.5) was found between DA amounts and late autophagy (anti-DA residual bodies) in the DG of the scallops.

Through the application of the specific IHC technique it was possible to detect a positive anti-DA chromogenic dying in some other tissues of highly contaminated scallops during both contamination and decontamination processes (Fig. 6). Toxin labeling was observed mainly in the microvilli of the branchial filaments (Fig. 6A), as well as in the axons and the somal body of the neurons embedded between the bundles of the adductor muscle (Fig. 6B). Moreover, anti-DA hues were also localized in the globose cells of the gonad ducts embedded in the male and female parts of the gonads of the scallops (Fig. 6C and D, respectively). Finally, no brown anti-DA signal was observed in the mantle or kidney of the scallops.

4. Discussion

A clear gap exists in knowledge about the physiological causes of the long retention of DA in king scallops *P. maximus*. The understanding of the biological mechanisms involved in both DA accumulation and depuration processes is of the utmost importance since the toxicity of scallop stocks during and after *Pseudo-nitzschia* blooms, and the kinetics of contamination and depuration of DA determines the consequent exploitation capacity of this resource. The ability to accumulate, retain, and redistribute DA burdens between different organs differs greatly between bivalve species (Blanco *et al.,* 2002b; Basti *et al.,* 2018). Furthermore, there is vast evidence that, in bivalves, DA depuration time is species-specific and has a wide range of variability. Most fast DA-depurators like mussels (Wohlgeschaffen *et al.* 1992; Novaczek *et al.,* 1992; Blanco *et al.* 2002b; Mafra *et al.,* 2010), many clams (Gilgan *et al.* 1990; Dusek Jennings *et al.,* 2020; Álvarez *et al.,* 2015; Blanco *et al.,* 2010), some oysters (Jones *et al.,* 1995; Mafra *et al.,* 2010), and even scallops (Álvarez *et al.,* 2020) are capable of detoxifying DA burdens up to 900 mg. kg^{-1} within hours or a few days, with detoxification rates ranging from 0.1 to ~ 2 day^{-1} in the whole body, and up to 10 day^{-1} in digestive tissues. Hence, retaining DA for a short time with a low impact on their harvest and commercialization.

Nonetheless, *P. maximus* is a particular case, since, as found in this work, the DA depuration rate calculated for the scallops in the digestive gland in this work was very low (0.001 day^{-1}) when compared to those of the bivalves mentioned above, but similar to that reported for the same species in the same organ by Blanco *et al.* (2002a, 2006) of about 0.003 and 0.007 day^{-1}, respectively. Notwithstanding, these depuration rates are too low even against those found in the digestive gland of other bivalves classified as slow DA-depurators as well, like *P. magellanicus* (~ 0.2 day^{-1}, Wohlgeschaffen *et al.,* 1992; Douglas *et al.,* 1997) and *S. patula* (0.05 and 0.02 day^{-1}, Horner *et al.,* 1993; Dusek Jennings *et al.,* 2020, respectively). Thus, demonstrating that *P. maximus* has the slowest DA-depuration kinetics among bivalves studied until now. In fact, using the depuration rate estimated in this study, it would take more than one year for the scallops of our experiment to almost depurate the total burdens of DA in the digestive gland. This duration is calculated under an environment virtually free of toxic *Pseudo-nitzschia*, which is practically impossible with the continuous presence of *P. australis* in the natural environment, as observed through the field monitoring in this work, and the repeated seasonal blooms of this species registered several times a year on the northwest coast of France (Amzil *et al.,* 2001; Husson *et al.,* 2016; Ayache *et al.,* 2019; REPHY-ifremer).

In this work, the DA contents measured in field-based scallops were the result of the continuously accumulated and subsequently depurated toxin. Therefore, differences in DA

accumulation-depuration in the organisms were strongly dependent on the toxicity of the *Pseudo-nitzschia* cells, the duration of the ASP blooms, the time through the animals were exposed to toxic microalgae and the moment at which the organisms were sampled during the bloom. This has a strong repercussion on the precision of the measurements of DA depuration rates in natural stocks. Therefore, it has to be taken into account during ASP-monitoring programs, either to avoid unnecessary fishery closures or to ensure public safety. To date, the only alternative for the profession to accelerate DA depuration of king scallops would be keeping contaminated animals in water systems free of toxic *Pseudo-nitzschia* during several months such as those used in this work for DA depuration, or the evisceration of the inedible and highly contaminated tissues (i.e. digestive gland) to reduce the toxin content of the product. Nevertheless, these solutions would not be economically feasible considering the space required for the conditioning of scallops, and the cost of such a procedures (F. Breton, *pers com,* 2023; Vanmaldergem *et al.,* 2023).

Moreover, there is a high inter-individual variability in the toxin burdens in the scallops. These large variations in DA contents, particularly in the DG (CV ranging from 30 to 125%) seem to be a characteristic of this species, as it was detected in several other studies (Blanco *et al.,* 2002a, 2006; Bogan *et al.*, 2007; García-Corona *et al.,* 2022). Nonetheless, the actual physiological reasons for these profound differences in DA accumulation/depuration rates between bivalves are still unclear. Recently, Alvarez *et al.* (2020) designed a multi-compartment model that suggests DA accumulated by *A. pupuratus* is rapidly transferred from the digestive gland to other organs such as the gonad, muscle, mantle, gills, but particularly the kidney, which depurate the toxin independently and with much more efficiency following a first-order exponential decay. The same strategy was proposed to explain the rapid detoxification of visceral DA in *Mytilus edulis* and *Crassostrea virginica* (Mafra *et al.,* 2010), as well as in *Mesodesma donacium* (Álvarez *et al.,* 2015) during early toxin uptake phase. Nonetheless, there is evidence that in the king scallop, DA redistribution from the digestive gland to other tissues, including the kidney, does not seem to occur, since previous findings demonstrate that the small fraction (≤ 5%) of total DA stored in the rest of the tissues is excreted at a rate 2.5-fold faster than in the digestive gland (Blanco *et al.,* 2002a, 2006). Throughout our monitoring of contamination and decontamination of the scallops, DA-staining in the rest of the tissues (gonad, muscle, gills, and gonads) was only observed in specific structures of the most contaminated scallops (~ 800-2000 mg DA kg^{-1}) in the entire study. The DA-signal was visualized in the microvilli of the gills and the globose cells

embedded in the spawning ducts of the gonads. A similar result was reported by García-Corona *et al.* (2022) in strongly DA-contaminated scallops *P. maximus*, where immunoreactivity occurred in mucus-producing structures. So far, it has not been confirmed whether DA has a simple chemical affinity to the mucus by some intermolecular forces, or if it is chemically bound to any component of the mucus. Nevertheless, as discussed above, since the amount of toxin in the rest of the tissues is negligible, it can be inferred that mucus production does not play an important role in toxin depuration in this species. Interestingly, DA IHC-staining was also found in the peripheral neural tissue of the scallops, particularly in the axon extensions and the soma body of some neurons embedded in the adductor muscle. The presence of high DA-affinity and low-sensitivity receptors has been identified in tissues of other bivalve species like *S. patula* (Trainer and Bill, 2004), which could indicate the presence of this type of receptors in *P. maximus*. Further studies are necessary to corroborate all these ideas.

As the digestive gland appeared as the key organ for the storage and depuration of DA in *P. maximus*, we focused on this organ to go deeper into the cause of the long retention of DA in *P. maximus.* No depuration of DA accumulated in the digestive gland of scallops was observed within the first 30 days of conditioning in the laboratory, with a slight reduction of DA burdens in this organ after 60 days of depuration. Our results put in evidence that during the period of active contamination, an intense process of early DA-autophagy was triggered, with the formation of autophagosomes in the apical region of the digestive cells cytoplasm, mainly within the digestive diverticula in absorptive and active digestion stages. According to Owen (1972) and Mathers (1976), this suggests an early and active assimilation of recently ingested food particles into the cells for digestion. Whereas the appearance of bigger autophagosomes in the distal cytoplasmic zone of digestive cells, such as those observed in the digestive diverticula in stages of advanced digestion, indicates the end of intracellular digestion or the early formation of residual bodies (Mathers, 1976; Yurchenko and Kalachev, 2019). On the other hand, the high intensity and prevalence of residual bodies with strong anti-DA signal widely distributed in digestive diverticula under breakdown or showing regeneration until the end of the depuration process reveal that DA is not completely excreted from the cells, remaining in the digestive gland for an indefinite time, as described in the literature (Owen, 1972; Cuervo, 2004; McMillan, 2018). This work constitutes evidence of the importance of autophagy in the toxicokinetics of DA in *P. maximus*. The long retention of exogenous compounds does not appear to be a phenomenon exclusively related to autophagy;

it also occurs in other types of cells under analogous cellular processes. Through macrophagy, specialized cells called macrophages use their cytoplasmic membranes to phagocytose large extracellular particles (≥ 0.5 μm, e.g. bacteria and metabolic debris) via endocytosis, creating internal vesicular compartments called phagosomes. Phagosomes with cargo materials fuse with lysosomes, forming phagolysosomes, leading to enzymatic degradation (Flannagan *et al.*, 2012; Gordon, 2016). There is evidence that, upon tattooing, mouse and human dermal macrophages are capable of: 1) phagocytosing pigment particles through several capture-release-recapture cycles across cell regeneration, or 2) exhibiting lifespans as long as the adult life of tattooed animals, accounting for both long-term persistence and strenuous removal of tattoo ink on the skin. Even when the macrophages laden with tattoo ink die and release the pigments, the staining particles remain in the extracellular space at the site of tattooing where they are recaptured by new macrophages (Baranska *et al.*, 2018). Like autophagy, macrophagy is a catabolic mechanism used to remove pathogens and cellular waste for detoxification or nutrient recycling purposes, in which macrophages can exhibit lifespans of months to years (Flannagan *et al.*, 2012; Gordon, 2016; Baranska *et al.*, 2018).

The results of this work and the discussed above suggest two new hypotheses: 1) DA may undergo successive cycles of capture–release–recapture by autophagosomic structures through the regenerative cycle of digestive cells of the scallops, or 2) autophagosomes and residual bodies with DA exhibit long lifespans without any toxin vanishing from months to years, thus triggering an analogous long-term DA-tattooing in the digestive glands of *P. maximus*. The direct and strong relationship found between early autophagy and DA accumulation, as well as the formation of residual bodies with depuration of the toxin denote that, at the subcellular level, autophagy could modulate the long-retention of DA in the digestive cells of *P. maximus*, by trapping the toxin and making it inaccessible to the detoxification system. The findings of this work are also reinforced by those of Ventoso *et al.* (2021) since the intramuscular injection of DA in *P. maximus* led to the overexpression of some genes related to autophagy and vesicle-mediated transport. Another question to be answered is the fate of the residual bodies with DA labeling after regeneration of digestive cells. Mathers (1976) demonstrated that the digestion cycle in the DG of *P. maximus* is closely correlated with the feeding tidal rhythm, where the intracellular digestion process of phagocytosed food materials is accomplished within a biphasic 12-h tidal cycle (24h total), including the formation of autophagosomes in cells showing active digestion, to the disintegration of residual bodies in the diverticula undergoing breakdown or showing

regeneration. The fact that DA is recognized by the anti-DA antibody despite several and relatively short time frames of cellular digestion mentioned before indicates the toxin is not being degraded. Therefore, the rapid cycles of cellular digestion are completely independent of the digestion, breakdown, and subsequent excretion of DA. This strengthens the DA-tattooing hypothesis proposed in this study, given the long persistence (up to several months) of DA-labeled autophagosomes and residual bodies observed in the digestive diverticula of *P. maximus* through the entire process of contamination and depuration of the toxin.

Conclusions

The *in situ* DA-immunodetection method applied in this work is a powerful tool to perform a subcellular time-tracking of domoic acid in tissues of king scallops during contamination and depuration phases. Early autophagy, with the formation of autophagosomes, appeared actively involved in the accumulation of the toxin in the digestive gland. This study also provides a strong presumption that the long retention of a portion of DA initially accumulated in king scallops is due to late autophagy, with the occurrence and long persistence of DA-labeled residual bodies, resembling an analogous DA-tattoo in the digestive gland of *P. maximus*. The quantitative immunohistochemical information developed in this work could be valuable for the development of numeric models that allow predicting the dynamics of contamination and decontamination with DA in natural fishery stocks. Moreover, our findings represent a cornerstone in the proposal of strategies to accelerate the depuration kinetics of ASP-toxin in this species.

Acknowledgments

The authors are deeply grateful to Sylvain Enguehard (Novakits, Nantes) for providing the non-commercial primary antibodies necessary to carry out this study, as well as Valentin Siebert, Erwan Amice, and Julien Thebault (LEMAR, Brest) for help with scallop collection. We also thank Margot Deleglise and Guillaume Bourhis, as well as all the Tinduff hatchery staff for assistance with scallop rearing overall the entire depuration experiment. We thank Marie Calvez, and Sébastien Artigaud (LEMAR, Brest) for assistance with tissue sectioning, and antibodies quantification, respectively, as well as Carmen Rodríguez-Jaramillo and Raúl Martínez-Rincón (CIBNOR, La Paz) for advices to optimize non-commercial antibodies for the IHC analysis, and for help improving R-scripts, respectively. Special thanks to Guadalupe Marrujo for sharing on her social media the article "Baranska *et al.*, 2018. Unveiling skin

macrophage dynamics explains both tattoo persistence and strenuous removal. *J Exp Med*" that inspired the DA-tattoo hypothesis in *P. maximus* of this work.

Declaration of competing interest

The authors declare that they have no known competing financial interests or personal relationships that could have appeared to influence the work reported in this paper.

Funding

This work received financial support from the research project “MaSCoET” (Maintien du Stock de Coquillages en lien avec la problématique des Efflorescences Toxiques) financed by France Filière Pêche and Brest Métropole, and from the project HIPPO financed by the Agence Nationale de la Recherche (grant no. ANR-18-CE92-0036-01). JLGC was recipient of a doctorate fellowship from CONACyT, Mexico (REF: 2019- 000025-01EXTF-00067), and JVM was financed by Actiris International European Youth Mobility Program.

Data availability statement

The evidence and data that support the findings of this study are available from the corresponding author upon reasonable request.

Ethics statements

The organisms used in this work were transported and handled according to the International Standards for the Care and Use of Laboratory Animals. The number of sampled animals contemplated "the rule of maximizing information published and minimizing unnecessary studies". In this sense, 126 scallops were considered the minimum number of organisms needed for this work.

Author contributions

Conceived the study: JLGC, HH, CF. Provided environmental data: AT, Performed the experiments: HH, JV, FB. Sampling: JLGC, JV, FB, CF, HH. Processed the samples: JLGC, JV, AD, SP, LB. Analyzed the data: JLGC, AD. Interpretation of data: JLGC, CF, HH. Contributed reagents/materials/analysis tools: CF, HH, AD, SP, FB. Wrote the first draft of the manuscript: JLGC. Writing – review & editing: CF, HH, JLGC.

Literature cited

556 Álvarez, G., Rengel, J., Araya, M., Álvarez, F., Pino, R., Uribe, E., Díaz, P.A., Rossignoli,
557 A.E., López-Rivera, A., Blanco, J., 2020. Rapid domoic acid depuration in the scallop
558 *Argopecten purpuratus* and its transfer from the digestive gland to other organs. *Toxins*,
559 12, 698. https://doi.org/10.3390/toxins12110698.

560 Álvarez, G., Uribe, E., Regueiro, J., Martin, H., Gajardo, T., Jara, L., Blanco, J., 2015.
561 Depuration and anatomical distribution of domoic acid in the surf clam *Mesodesma*
562 *donacium*. *Toxicon*, 102, 1–7. https://doi.org/10.1016/j.toxicon.2015.05.011.

563 Amzil, Z., Fresnel, J., Le Gal, D., Billard, C., 2001. Domoic acid accumulation in French
564 shellfish in relation to toxic species of *Pseudo-nitzschia multiseries* and *P.*
565 *pseudodelicatissima*. *Toxicon*, 39(8), 1245–1251. https://doi.org/10.1016/s0041-
566 0101(01)00096-4.

567 Ayache, N., Hervé, F., Lundholm, N., Amzil, Z., & Caruana, A. M. N., 2019. Acclimation of
568 the Marine Diatom *Pseudo- nitzschia australis* to Different Salinity Conditions: Effects on
569 Growth, Photosynthetic Activity, and Domoic Acid Content. In T. Mock (Ed.), Journal of
570 Phycology (Vol. 56, Issue 1, pp. 97–109). Wiley. https://doi.org/10.1111/jpy.12929.

571 Baranska, A., Shawket, A., Jouve, M., Baratin, M., Malosse, C., Voluzan, O., Vu Manh, T.-
572 P., Fiore, F., Bajénoff, M., Benaroch, P., Dalod, M., Malissen, M., Henri, S., Malissen, B.,
573 2018. Unveiling skin macrophage dynamics explains both tattoo persistence and strenuous
574 removal. *Journal of Experimental Medicine*, 215(4), 1115–1133.
575 https://doi.org/10.1084/jem.20171608.

576 Basti, L., Hégaret, H., Shumway, S.E. 2018. Harmful Algal Blooms and Shellfish. In:
577 Harmful Algal Blooms: A Compendium Desk Reference, First Edition. Shumway, S.E.,
578 Burkholder, J.M., Morton, S.L. (eds). John Wiley & Sons Ltd.

579 Bates, S.S., Hubbard, K.A., Lundholm, N., Montresor, M., Leaw, C.P. 2018. *Pseudo-*
580 *nitzschia, Nitzschia*, and domoic acid: new research since 2011. *Harmful Algae*, 79, 3-43.
581 https://doi.org/10.1016/j.hal.2018.06.001.

582 Blanco, J., Acosta, C., Bermúdez de la Puente, M., Salgado, C., 2002a. Depuration and
583 anatomical distribution of the amnesic shellfish poisoning (ASP) toxin domoic acid in the
584 king scallop *Pecten maximus*. *Aquatic Toxicology*, 60 (1-2), 111–121.
585 https://doi.org/10.1016/s0166-445x(01)00274-0.

586 Blanco, J., Acosta, C.P., Mariño, C., Muñiz, S., Martín, H., Moroño, A., Correa, J., Arévalo,
587 F., Salgado, C., 2006. Depuration of domoic acid from different body compartments of the
588 king scallop *Pecten maximus* grown in raft culture and natural bed. *Aquatic Living*
589 *Resources*, 19 (3), 257–265. https://doi.org/10.1051/alr:2006026.

590 Blanco, J., Bermúdez, M., Arévalo, F., Salgado, C., Moroño, A., 2002b. Depuration of
591 mussels (*Mytilus galloprovincialis*) contaminated with domoic acid. *Aquatic Living*
592 *Resources*, 15, 53–60. https://doi.org/10.1016/S0990-7440(01)01139-1.

Blanco, J., Livramento, F., Rangel, I. M., 2010. Amnesic shellfish poisoning (ASP) toxins in plankton and molluscs from Luanda Bay, Angola. *Toxicon*, 55(2–3), 541–546. https://doi.org/10.1016/j.toxicon.2009.10.008.

Blanco, J., Mauríz, A., Álvarez, G., 2020. Distribution of Domoic Acid in the Digestive Gland of the King Scallop *Pecten maximus*. *Toxins*, 12(6), 371. https://doi.org/10.3390/toxins12060371.

Bogan, Y. M., Kennedy, D. J., Harkin, A. L., Gillespie, J., Vause, B. J., Beukers-Stewart, B. D., Hess, P., Slater, J.W., 2007. Variation in domoic acid concentration in king scallop (*Pecten maximus*) from fishing grounds around the Isle of Man. *Harmful Algae*, 6, 81–92. https://doi.org/10.1016/j.hal.2006.07.002.

Bresnan, E., Fryer, R. J., Fraser, S., Smith, N., Stobo, L., Brown, N., & Turrell, E., 2017. The relationship between *Pseudo-nitzschia* (Peragallo) and domoic acid in Scottish shellfish. Harmful Algae, 63: 193–202. https://doi.org/10.1016/j.hal.2017.01.004.

Cuervo, A.M., 2004. Autophagy: many paths to the same end. *Molecular and Cellular Biochemistry*, 263 (1/2), 55–72. https://doi.org/10.1023/b:mcbi.0000041848.57020.57.

Douglas, D.J., Kenchington, E.R., Bird, C.J., Pocklington, R., Bradford, B., Silvert, W. 1997. Accumulation of domoic acid by the sea scallop (*Placopecten magellanicus*) fed cultured cells of toxic *Pseudo-nitzschia multiseries*. *Canadian Journal of Fisheries and Aquatic Sciences*, 54 (4), 907–913. https://doi.org/10.1139/f96-333.

Drum, A.S., Siebens, T.L., Crecelius, E.A., Elston, R.A. 1993. Domoic acid in the Pacific razor clam *Siliqua patula* (Dixon, 1789). *Journal of Shellfish Research*, 12, 443–450.

Dusek Dusek Jennings, E., Parker, M. S., Simenstad, C. A., 2020. Domoic acid depuration by intertidal bivalves fed on toxin-producing *Pseudo-nitzschia multiseries*. *Toxicon*, 6, 100027. https://doi.org/10.1016/j.toxcx.2020.100027.

Flannagan, R. S., Jaumouillé, V., Grinstein, S., 2012. The Cell Biology of Phagocytosis. *Annual Review of Pathology: Mechanisms of Disease*, 7(1), 61–98. https://doi.org/10.1146/annurev-pathol-011811-132445.

García-Corona, J. L., Hégaret, H., Deléglise, M., Marzari, A., Rodríguez-Jaramillo, C., Foulon, V., Fabioux, C., 2022. First subcellular localization of the amnesic shellfish toxin, domoic acid, in bivalve tissues: Deciphering the physiological mechanisms involved in its long-retention in the king scallop *Pecten maximus*. *Harmful Algae*, 116. https://doi.org/10.1016/j.hal.2022.102251.

García-Corona, J.L., Hegaret, H., Lassudrie-Duchesne, M., Derrien, A., Terre-Terrillon, A., Delaire, T., Fabioux, C. 2023. Comparative study of domoic acid accumulation, isomer content and associated digestive subcellular processes in five marine invertebrate species. *Aquatic toxicology*, 266, 106793. https://doi.org/10.1016/j.aquatox.2023.106793.

Gilgan, M.W., Burns B.G., Landry, G.J., 1990. Distribution and magnitude of domoic acid contamination of shellfish in Atlantic Canada. In: E. Graneli, B. Sundstrom, L. Edler, D.M. Anderson (Eds.), Toxic Marine Phytoplankton. Elsevier, N.Y. pp. 469- 474.

Gordon, S., 2016. Phagocytosis: An Immunobiologic Process. *Immunity*, 44(3), 463–475. https://doi.org/10.1016/j.immuni.2016.02.026.

Hallegraeff, G. M. (1993). A review of harmful algal blooms and their apparent global increase. In Phycologia (Vol. 32, Issue 2, pp. 79–99). Informa UK Limited. https://doi.org/10.2216/i0031-8884-32-2-79.1.

Hector, A., 2015. The new statistics with R: an introduction for biologists, 1st ed. Oxford University Press, New York.

Horner, R.A., Kusske, M.B., Moynihan, B.P., Skinner, R.N., Wekell, J.C., 1993. Retention of Domoic Acid by Pacific Razor Clams, *Siliqua patula* (Dixon, 1789): Preliminary Study. *Journal of Shellfish Research*, 12, 451–456.

Husson, B., Hernández-Fariñas, T., Le Gendre, R., Schapira, M., Chapelle, A., 2016. Two decades of *Pseudo-nitzschia spp*. blooms and king scallop (*Pecten maximus*) contamination by domoic acid along the French Atlantic and English Channel coasts: Seasonal dynamics, spatial heterogeneity and interannual variability. *Harmful Algae*, 51, 26–39. https://doi.org/10.1016/j.hal.2015.10.017

Jones, T.O., Whyte, J.N.C., Ginther, N.G., Townsend, L.D., Iwama, G.K., 1995. Haemocyte changes in the pacific oyster, *Crassostrea gigas*, caused by exposure to domoic acid in the diatom *Pseudo-nitzschia pungens* f. multiseries. *Toxicon*, 33 (3), 347–353. https://doi.org/10.1016/0041-0101(94)00170-.

Kim, Y., Ashton-Alcox, K.A., Powell, E.N., 2006. Histological Techniques for Marine Bivalve Molluscs: update. NOAA Technical Memorandum NOS NCCOS 27, Maryland.

La Barre, S., Bates, S.S. Quilliam, M.A. 2014. Domoic acid. In. Outstanding marine molecules: chemistry, biology, analysis. Edited by S. La Barre and J.-M. Kornprobst. Wiley-VCH Verlag GmbH & Co. KgaA, Weinheim, Germany, pp. 189–216.

Lelong, A., Hégaret, H., Soudant, P., Bates, S.S. 2012. *Pseudo-nitzschia* (Bacillariophyceae) species, domoic acid and amnesic shellfish poisoning: revisiting previous paradigms. *Phycologia*, 51 (2), 168–216. https://doi.org/10.2216/11-37.1.

MacKenzie, J.D., Bavington, C, 2002). Measurement of Domoic Acid in King Scallops processed in Scotland. Final Report for The Food Standards Agency Scotland. https://www.foodstandards.gov.scot/downloads/Domoic_Acid_in_King_Scallops.pdf.

Mafra, L.L., Bricelj, V.M., Fennel, K., 2010. Domoic acid uptake and elimination kinetics in oysters and mussels in relation to body size and anatomical distribution of toxin. *Aquatic Toxicology*, 100 (1), 17–29. https://doi.org/10.1016/j.aquatox.2010.07.0.

Mathers, N.F., 1976. The effects of tidal currents on the rhythm of feeding and digestion in Pecten maximus L. *Journal of Experimental Marine Biology and Ecology*, 24 (3), 271–283. https://doi.org/10.1016/0022-0981(76)90059-9.

Mauríz, A., Blanco, J., 2010. Distribution and linkage of domoic acid (amnesic shellfish poisoning toxins) in subcellular fractions of the digestive gland of the scallop *Pecten maximus*. *Toxicon*, 55 (2-3), 606–611. https://doi.org/10.1016/j.toxicon.2009.10.

McMillan, D.B., Harris, R.J., 2018. The Animal Cell. In An Atlas of Comparative Vertebrate Histology (pp. 3–25). Elsevier. https://doi.org/10.1016/b978-0-12-410424-2.00001-9.

Mizushima, N., Ohsumi, Y., & Yoshimori, T., 2002. Autophagosome Formation in Mammalian Cells. *Cell Structure and Function*, 27(6): 421–429. https://doi.org/10.1247/csf.27.421.

Moore, M.N., 2004. Diet restriction induced autophagy: a lysosomal protective system against oxidative- and pollutant-stress and cell injury. *Marine Environmental Research*, 58 (2–5), 603–607. https://doi.org/10.1016/j.marenvres.2004.03.

Novaczek, I., Madhyastha, M.S., Ablett, R.F., Donald, A., Johnson, G., Nijjar, M.S., Sims, D.E., 1992. Depuration of domoic acid from live blue mussels (*Mytilus edulis*). *Canadian Journal of Fisheries and Aquatic Sciences*, 49 (2), 312–318. https://doi.org/10.1139/f92-035.

Owen, G., 1972. Lysosomes, peroxisomes and bivalves. Science Progress 60 (239), 299–318.

Picot, S., Morga, B., Faury, N., Chollet, B., Dégremont, L., Travers, M.A., Renault, T., Arzul, I., 2019. A study of autophagy in hemocytes of the Pacific oyster *Crassostrea gigas*. *Autophagy*, 1–9. https://doi.org/10.1080/15548627.2019.1596.

Pulido, O.M. 2008. Domoic Acid Toxicologic Pathology: A Review. *Marine Drugs*, 6, 180-219. https://doi.org/10.3390/md20080010.

Quilliam, M.A., Sim, P.G., McCulloch, A.W., McInnes, A.G., 1989. High-performance liquid chromatography of domoic acid, a marine neurotoxin, with application to shellfish and plankton. *International Journal of Environmental Analytical Chemistry*, 36 (3), 139–154. https://doi.org/10.1080/03067318908026867.

R Core Team (2020). R: a language and environment for statistical computing. R Foundation for Statistical Computing, Vienna, Austria. URL https://www.R-project.org/.

REPHY - French Observation and Monitoring program for Phytoplankton and Hydrology in coastal waters (2022). REPHY dataset - French Observation and Monitoring program for Phytoplankton and Hydrology in coastal waters. Metropolitan data. SEANOE. https://doi.org/10.17882/47248.

Trainer, V.L., Bates, S.S., Lundholm, N., Thessen, A.E., Cochlan, W.P., Adams, N.G., 2012. *Pseudo-nitzschia* physiological ecology, phylogeny, toxicity, monitoring and impacts on ecosystem health. *Harmful Algae*, 14, 271–300. https://doi.org/10.1016/j.hal.2011.10.025.

Trainer, V.L., Bill, B.D., 2004. Characterization of a domoic acid binding site from Pacific razor clam. *Aquatic Toxicology*, 69, 125–132. https://doi.org/10.1016/j.aquatox.2004.04.012.

Vanmaldergem, J., García-Corona, J. L., Deléglise, M., Fabioux, C., Hegaret, H., 2023. Effect of the antioxidant N-acetylcysteine on the depuration of the amnesic shellfish poisoning toxin, domoic acid, in the digestive gland of the king scallop *Pecten maximus*. *Aquatic Living Resources*, 36, 14. https://doi.org/10.1051/alr/2023011.

Ventoso, P., Pazos, A.J., Blanco, J., Pérez-Parallé, M.L., Triviño, J.C., Sánchez, J.L., 2021. Transcriptional Response in the Digestive Gland of the King Scallop (*Pecten maximus*) After the Injection of Domoic Acid. *Toxins*, 13, 339. https://doi.org/10.3390/toxins13050339.

Wang, L., Ye, X., Zhao, T., 2019. The physiological roles of autophagy in the mammalian life cycle. *Biological Reviews*, 94, 503–516. https://doi.org/10.1111/brv.12464.

Wekell, J. C., Hurst, J., & Lefebvre, K. A., 2004. The origin of the regulatory limits for PSP and ASP toxins in shellfish. Journal of Shellfish Research, 23(3), 927.

Wohlgeschaffen, G.D., Mann, K.H., Subba Rao, D.V., Pocklington, R. 1992. Dynamics of the phycotoxin domoic acid: accumulation and excretion in two commercially important bivalves. *Journal of Applied Phycology*, 4(4), 297–310. https://doi.org/10.1007/bf02185786.

Yurchenko, O., Kalachev, A., 2019. Morphology of nutrient storage cells in the gonadal area of the Pacific oyster, *Crassostrea gigas* (Thunberg, 1793). Tissue Cell 56, 7–13. https://doi.org/10.1016/j.tice.2018.11.004.

Zar, J. H., 2010. Biostatistical Analysis. 5th Ed. Pearson, Westlake Village, CA, 251 pp.

Zhao, Y.G., Codogno, P., Zhang, H., 2021. Machinery, regulation and pathophysiological implications of autophagosome maturation. *Nature Reviews Molecular Cell Biology*. https://doi.org/10.1038/s41580-021-00392-4.

Zheng, G., Wu, H., Guo, M., Peng, J., Zhai, Y., Tan, Z., 2022. First observation of domoic acid and its isomers in shellfish samples from Shandong Province, China. *Journal of Oceanology and Limnology*, 40(6) 2231–2241. https://doi.org/10.1007/s00343-022-2104-3.

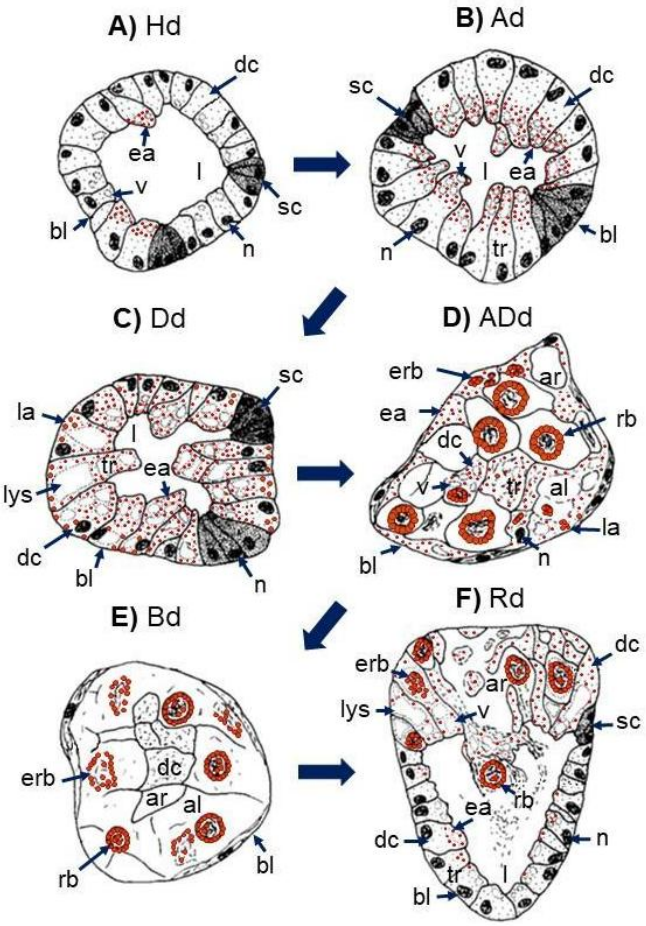

731

732 **Figure 1.** Transversal diagrammatic illustrations of the digestive diverticula (dd) in the
733 digestive gland (DG) of *P. maximus* during a digestive cycle. (A) digestive diverticulum in a
734 holding condition (Hd); cubical digestive cells (dc) with few vacuoles (v) and almost no
735 autophagosomes line a large lumen (l) and secretory cells (sc) are easily identified. (B)
736 diverticulum in absorptive condition (Ad); vacuoles and small early autophagosomes are
737 present in the apical region of the digestive cells. (C) diverticulum in digestive condition
738 (Dd); early autophagosomes (ea) are widely distributed throughout the digestive cells in the
739 tubular region; basal vacuoles or lysosomes (lys) are identified, few bigger late
740 autophagosomes (la) are present in the basal region of the cytoplasm. (D) diverticulum in
741 advance digestive condition (ADd); secretory cells are absent, digestive cells in the tubular
742 region are filled with early autophagosomes in the apical region and late autophagosomes in
743 the basal region of the cytoplasm, while early residual bodies (erb) and residual bodies (rb) in
744 are visualized in the adipocyte-like cells (al). (E) diverticulum undergoing breakdown;
745 digestive cells show loss of structure and form, high presence of residual bodies (rb) in the
746 ascinar region (ar) within abundant adipocyte-like cells. (F) diverticulum showing
747 regeneration; the secretory cells are again visible at the junctions between the old (ascinar
748 region) and new (tubular region) diverticulum, early autophagosomes present in the apical
749 region, and late autophagosomes in the basal region of digestive cells, presence of residual
750 bodies in adipocyte-like cells. bl = basal lamina, n = nucleus. Modified from Mathers (1976)
751 indicating the localization of DA in the digestive glands of *P. maximus*.

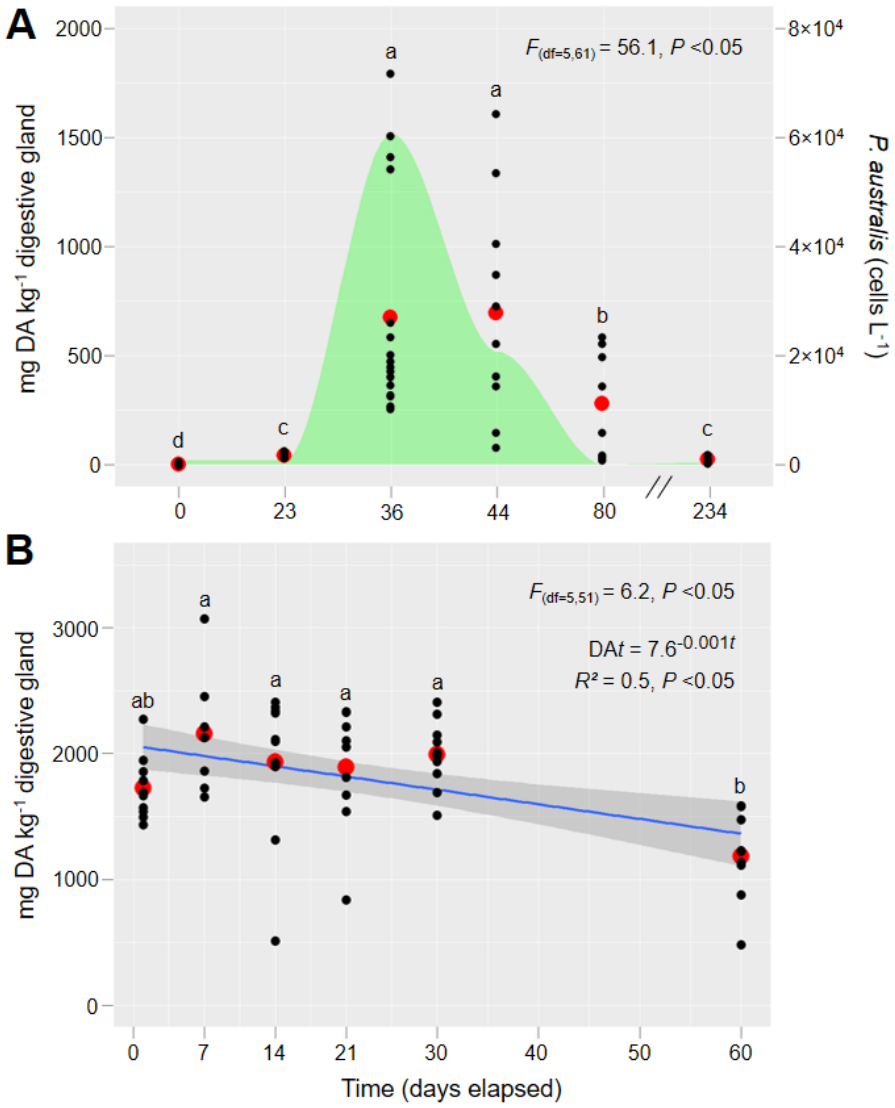

Figure 2. Concentrations of DA in the digestive glands of scallops *P. maximus* (A) during natural contamination process during outbreak of the toxic *Pseudonitzschia australis* in the northwest coast of France between February and October 2021, and (B) during the DA-depuration in the laboratory for 60 days after a natural DA-contamination event during toxic *Pseudo-nitzschia spp.* outbreak in the northwest coast of France in April 2021. The black dots are the individual observations, and red dots are the means. (A) The green shaded area corresponds to the cell densities of *P. australis* in the field. (B) The daily DA depuration rate was calculated using the one-compartment exponential decay model, $DA_t = DA_0 \cdot e^{-rt}$, where DA_t is the DA concentration after t days, DA_0 represents DA concentration at the end of the depuration, t is days elapsed, and the slope of the equation (r) is the daily depuration rate. DA_0 and the slope were estimated using linear regression (blue line, R^2 ± standard deviation) after ln-transformation of DA burdens, but untransformed data are presented. Data on DA concentrations were analyzed using the sampling time (six levels) as independent variable in separate one-way ANOVA's. The F-test statistic and degrees of freedom (df) are reported. Different superscript letters denote statistically significant differences between groups. The level of statistical significance was set at $\alpha = 0.05$.

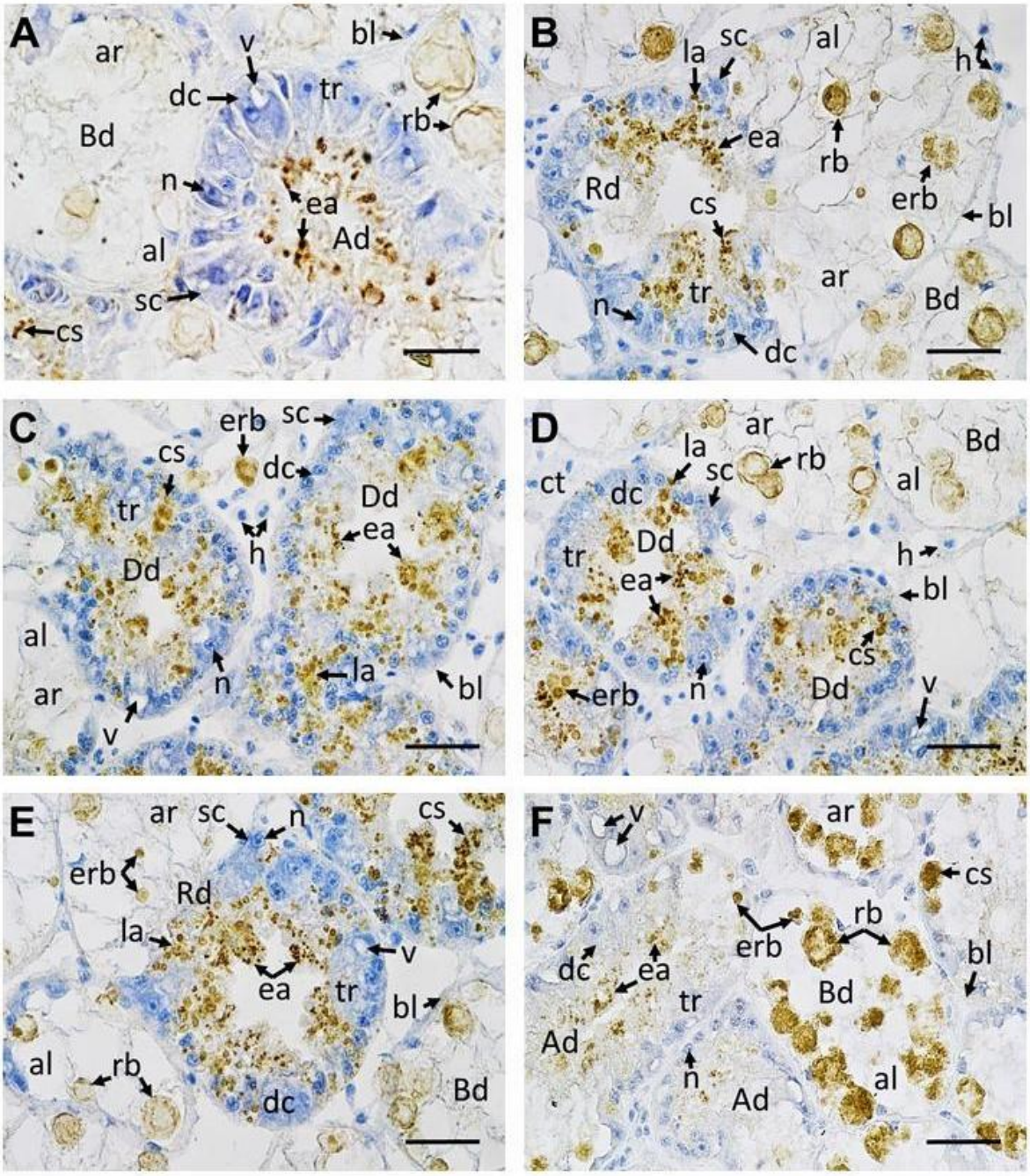

Figure 3. Microphotographs of digestive glands of scallops *P. maximus* during a natural process of DA-contamination during outbreaks of the toxic *P. australis*in the northwest coast of France between February and October 2021. A) Day 0, B) Day 23, C) Day 36, D) Day 44, E) Day 80, F) Day 234. Specific anti-DA immunohistochemical (IHC) staining appeared in brown. Ad = digestive diverticulum in absorptive condition, ADd = digestive diverticulum in advanced digestive condition, al = adipocyte-like digestive cell, ar = acinar region, Bd = digestive diverticulum undergoing breakdown, bl = basal lamina, cs = positive anti-DA chromogenic signal, ct = connective tissue, dc = digestive cells, Dd = digestive diverticulum in digestive condition, ea = early-autophagosomes, erb = early- residual bodies, h = hemocytes, la = late-autophagosomes, n = nucleus, rb = residual bodies, Rd = diverticulum showing regeneration, tr = tubular region. Scale bar: 63 × = 30 µm.

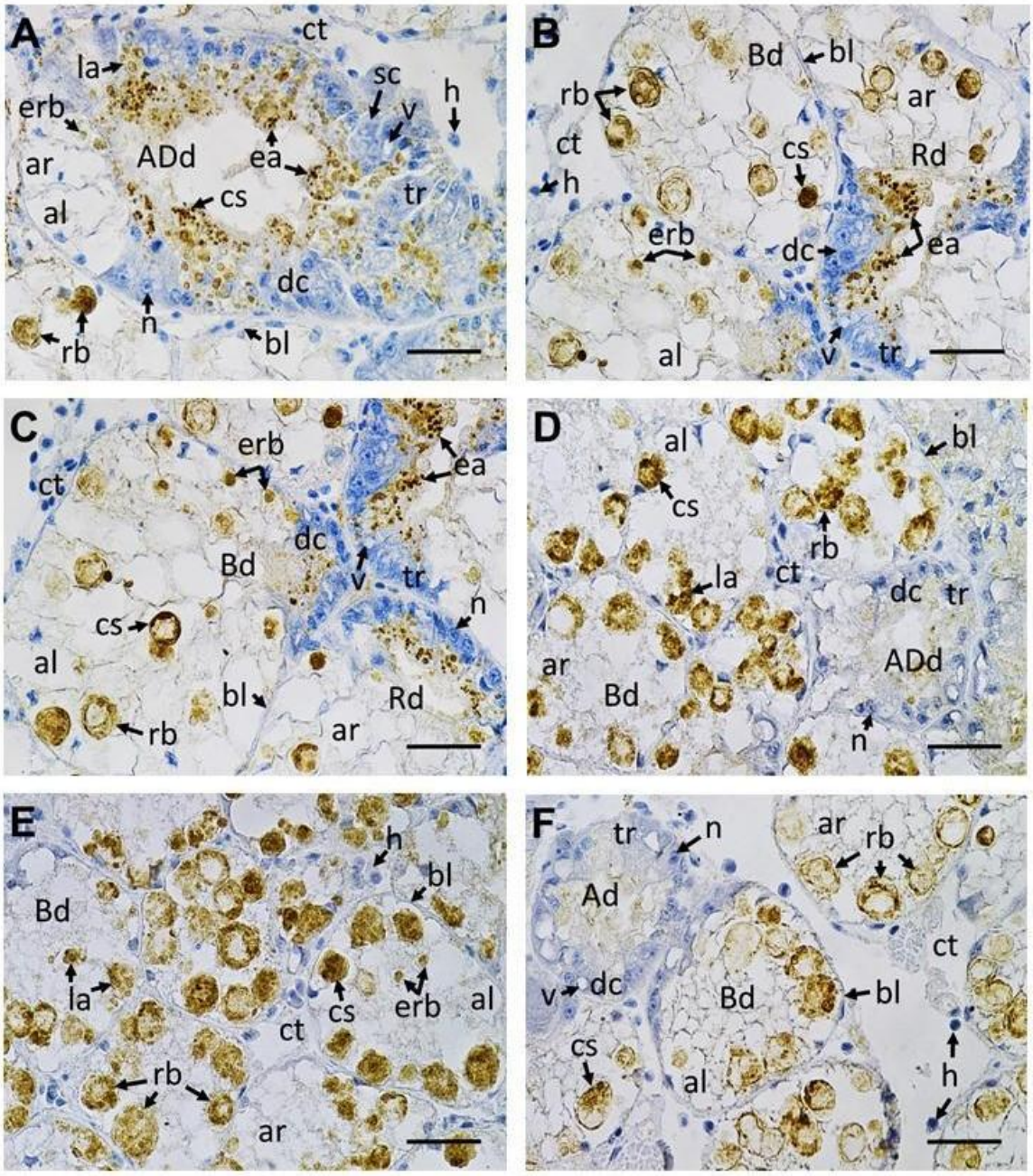

781

782 **Figure 4.** Microphotographs of digestive glands of naturally DA-contaminated scallops *P.*
783 *maximus* collected after outbreaks of toxic *Pseudo-nitzschia spp.* in the northwest coast of
784 France in early April 2021 and subjected to DA-depuration in the laboratory for 60 days. A)
785 Day 0, B) Day 7, C) Day 14, D) Day 21, E) Day 30, F) Day 60. Specific anti-DA
786 immunohistochemical (IHC) staining incubated with the primary and secondary antibodies
787 (0.01 mg. mL^{-1} and 0.001 mg mL^{-1}, respectively). Ad = digestive diverticulum in absorptive
788 condition, ADd = digestive diverticulum in advanced digestive condition, al = adipocyte-like
789 digestive cell, ar = acinar region, Bd = digestive diverticulum undergoing breakdown, bl =
790 basal lamina, cs = positive anti-DA chromogenic signal, ct = connective tissue, dc = digestive
791 cells, Dd = digestive diverticulum in digestive condition, ea = early-autophagosomes, erb =
792 early- residual bodies, h = hemocytes, la = late-autophagosomes, n = nucleus, rb = residual
793 bodies, Rd = diverticulum showing regeneration, tr = tubular region. Scale bar: 63 × = 30 µm.

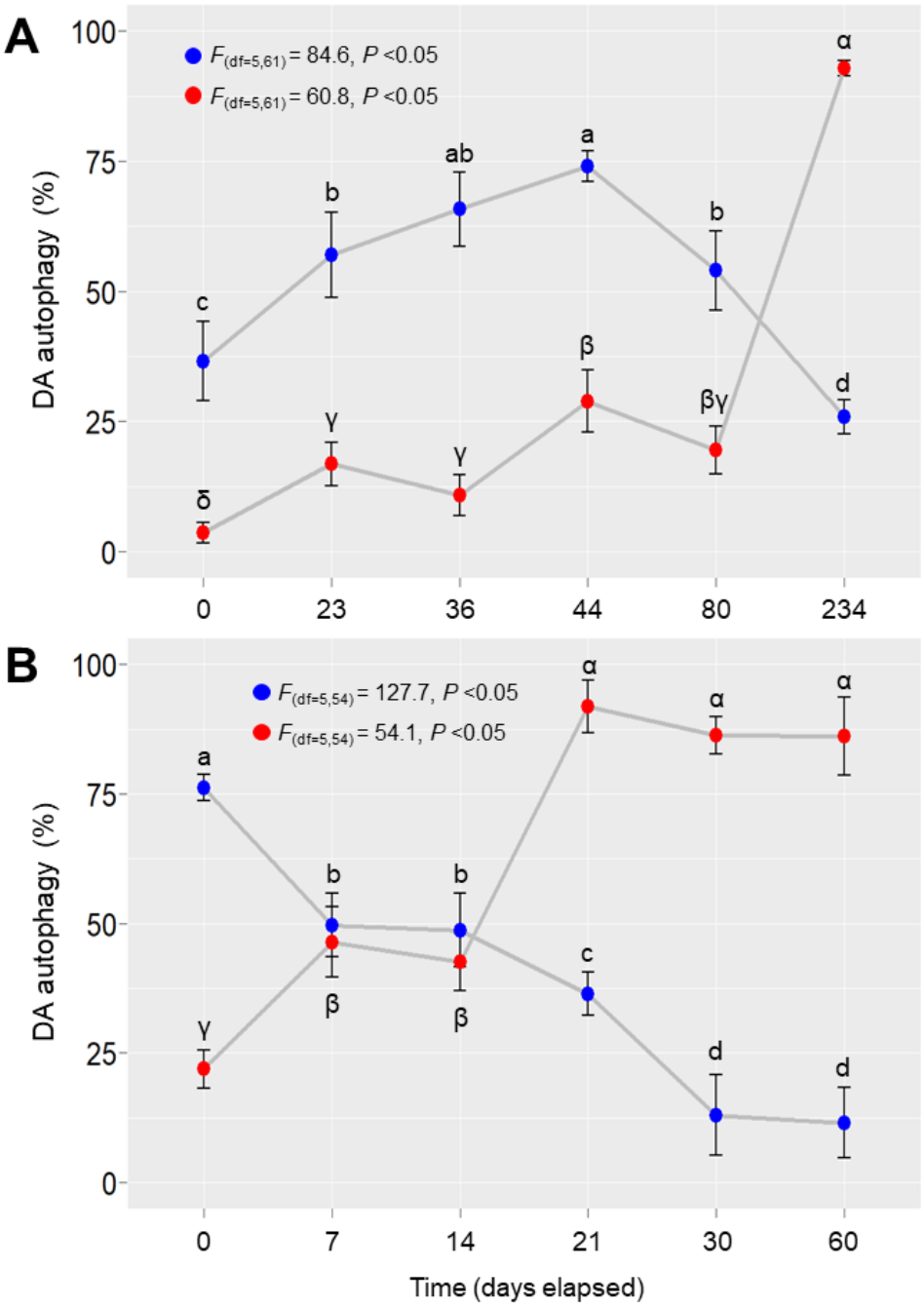

Figure 5. DA autophagy (%) in the digestive gland of scallops *P. maximus* (A) naturally contaminated during outbreaks of the toxic *P. australis* in the northwest coast of France between February and October 2021, and (B) naturally contaminated scallops *P. maximus* collected after outbreaks of toxic *Pseudo-nitzschia spp.* in the northwest coast of France in April 2021 and subjected to DA-depuration in the laboratory for 60 days. The blue dots (early-autophagy = autophagosomes) and red dots (late-autophagy = residual bodies) are the means. Results are expressed as mean ± SE. Data were analyzed using the sampling time (six levels) as independent variable in separate one-way ANOVA's. The *F*-test statistic and degrees of freedom (*df*) are reported. Different superscript letters denote statistically significant differences between groups. The level of statistical significance was set at α = 0.05.

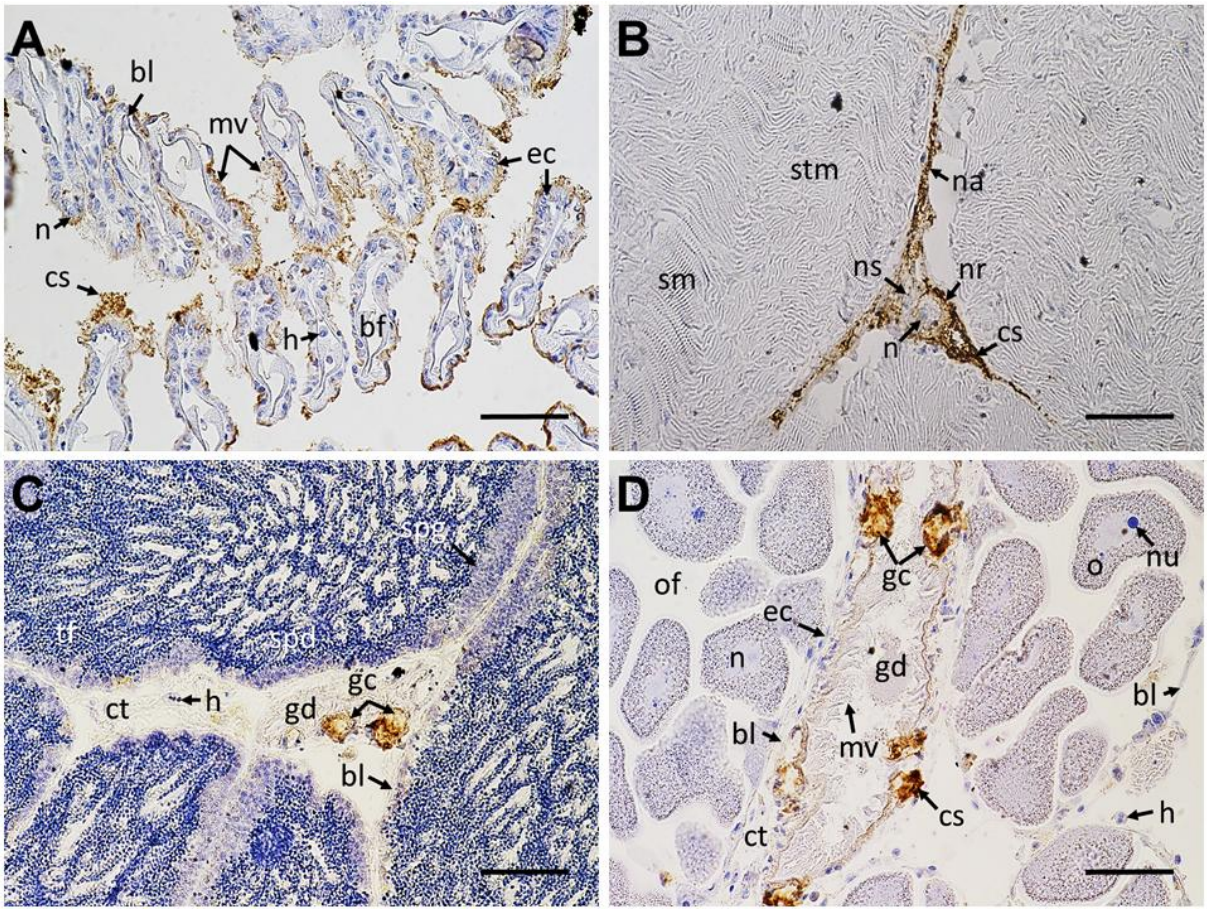

806

807 **Figure 6.** Microphotographs of the rest of tissues (A, gills; B, adductor muscle; C, male
808 gonad; D, female gonad) of highly DA-contaminated (~ 800-2000 mg DA kg^{-1}) scallops *P.*
809 *maximus*. Specific anti-DA immunohistochemical (IHC) staining appeared in brown hues on
810 the images. bf = branchial filament, bl = basal lamina, cs = positive anti-DA chromogenic
811 signal, ct = connective tissue, ec = epithelial cell, gc = globose cell, gd = gonadal duct, h =
812 hemocytes, mv = microvilli, n = nucleus, na = neuronal axon, nr = neuron, ns = neuronal
813 soma, nu = nucleolus, o = oocyte, of = ovarian follicle, sm = striated muscle, spd =
814 spermatids, spg = spermatogonia, stm = smooth muscle, tf = testicular follicle. Scale bar: 40 ×
815 = 50 µm.